Hole doping effect on superconductivity in $Ce(Co_{1-x}Ru_x)In_5$

M. N. Ou,[1,2,*] K. Gofryk,[1] R. E. Baumbach,[1] S. S. Stoyko,[3] J. D. Thompson,[1] J. M. Lawrence,[1] E. D. Bauer,[1] F. Ronning,[1] A. Mar,[3] and Y. Y. Chen[2,†]

[1]*Los Alamos National Laboratory, Los Alamos, New Mexico 87545, USA*

[2]*Institute of Physics, Academia Sinica, Taipei 11529, Taiwan*

[3]*Department of Chemistry, University of Alberta, Edmonton, Canada T6G 2G2*

(Received 19 July 2013; revised manuscript received 17 October 2013; published 19 November 2013)

$CeCoIn_5$, which has a superconducting transition temperature of 2.3 K, provides an excellent opportunity to study the interplay of superconductivity and magnetism near an antiferromagnetic quantum critical point. Previous studies have explored the effects of electron doping, magnetic field, and positive pressure on this system. To determine the effect of hole doping, we have grown single crystals of $Ce(Co_{1-x}Ru_x)In_5$ in indium flux. The crystal structure of these Ru-doped samples was identified by powder XRD as the $HoCoGa_5$-type. We find that the coherence temperature T^* and the superconducting transition temperature T_c decrease monotonically with increasing Ru content. Unlike the case of hole doping in $CeCo(In_{5-x}Cd_x)$ alloys in which antiferromagnetism starts to emerge at $x = 0.025$, we find no magnetic transition at our maximal nominal doping of $x_{nom} = 0.5$, where T_c is suppressed to 1.5 K. We discuss possible reasons for this difference between these two cases of hole doping.

DOI: 10.1103/PhysRevB.88.195134 PACS number(s): 71.27.+a, 74.70.Tx, 72.15.Qm, 75.30.Mb

I. INTRODUCTION

An important issue in the study of strongly correlated electron systems (SCES) is the competition between Fermi liquid, antiferromagnetic (AFM), and unconventional superconducting (SC) ground states. Heavy fermion systems are ideal compounds for investigating how these phases emerge near an AFM quantum critical point (QCP).[1] Various external parameters such as composition (x), pressure (P), and magnetic field (H) are used to tune among these ground states. Previous work[2] shows that the QCP can be attained by alloying in $Ce(Cu_{6-x}Au_x)$, while studies[3] of $CeIn_3$ and $CePd_2Si_2$ under application of pressure suggest that a narrow superconducting dome may emerge near the AFM QCP.

The compounds $CeMIn_5$ (M = Rh, Ir, Co) exhibit low-temperature behavior that appears to be strongly influenced by proximity to a quantum critical point in T-x-P-H phase space and hence provide a convenient stage for the study of quantum criticality (QC) near an AFM QCP. These compounds form in the tetragonal $HoCoGa_5$ ($P4/mmm$) structure where a MIn_2 buffer layer is sandwiched between two active $CeIn_3$ layers.[4] The ground state of these 1-1-5 compounds can be tuned by isoelectronic doping[5,6] between SC states in $CeCoIn_5$ ($T_c = 2.3$ K) and $CeIrIn_5$ ($T_c = 0.4$ K) and an AFM state in $CeRhIn_5$ ($T_N \sim 4$ K). Experimental results suggest that $CeCoIn_5$(Co115) is located very close to an AFM QCP.[7,8] A number of studies of doping onto the Ce and In sites in Co115 have been performed in order to probe QC near an AFM QCP.[9–13] The correlated electron effects are only weakly affected by Yb substitution onto the Ce site, while they are strongly affected by other rare earths.[14,15] Recent results for Co115 show that electron doping by substitution of Pt onto the Co site or Sn onto the In site drives the system away from the QCP into a less-enhanced Fermi liquid state while hole doping with Cd or Hg onto the In site drives the system through the QCP into an AFM state. Moreover, the effects of hole doping through substitution of Hg in this compound can be reversed by electron doping through additional substitution of Pt or Sn.[16,17]

II. EXPERIMENT

In this paper, we report investigations of the effect of hole doping by substitution of ruthenium onto the Co site. Five batches of $Ce(Co_{1-x}Ru_x)In_5$ with nominal (starting) doping concentrations of x_{nom} = 0.1, 0.2, 0.3, 0.4, and 0.5 were synthesized by means of the self-flux method in an indium solvent.[7,18,19] The crystals grew in the tetragonal $HoCoGa_5$ structure, forming flat sheets with dimensions of order of 1 mm in width and length and 100 μm in thickness. The x-ray diffraction (XRD) rocking scan revealed that the [001] direction was perpendicular to the plane of each individual plate. The $HoCoGa_5$ structure was found to exist only for concentrations less than a maximum nominal concentration x_{nom}= 0.5; for larger concentrations, the resulting crystals were found to crystallize in the Ce_2CoIn_8 structure with major inclusions of $RuIn_3$. Refinement of both single crystal and polycrystalline XRD profiles (where the polycrystal samples were formed by powdering selected crystals) showed that the lattice volume expanded slightly as the doping level increased up to $x_{nom} = 0.3$, and then was constant in the range $0.3 < x_{nom} < 0.5$ [see Fig. 1(a)]. The maximum increase of lattice constants for both the a and c axes is of order 0.3%. For $0 \leqslant x_{nom} \leqslant 0.3$, the average concentration x_{av}(XRD) of Ru as determined from refinement of the single crystal samples was found to be 3–4 times smaller than x_{nom}, while for larger x_{nom}, the average concentration appears to saturate [see Fig. 1(b)]. Energy-dispersive x-ray (EDX) analyses were performed on a JEOL JSM-6010LA scanning electron microscope operated with an accelerating voltage of 20 kV. Each crystal was examined on at least two different areas, with between 12 to 30 points analyzed for each area over an acquisition time of 60 seconds per point. Secondary electron and backscattered

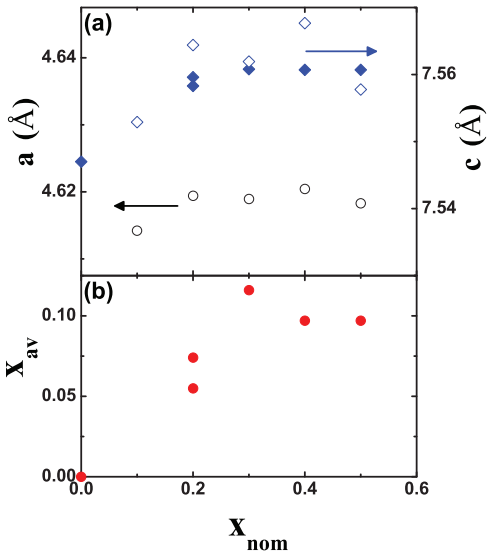

FIG. 1. (Color online) XRD analysis of a series of $Ce(Co_{1-x}Ru_x)In_5$ alloys with nominal concentration in the range $x_{nom} = 0.1$ to 0.5. Closed symbols correspond to single crystal data; open symbols to powder diffraction. (a) The lattice constants and (b) the average Ru concentration deduced from refinement of single crystal profiles.

electron images were also acquired for all crystals. The EDX diffraction revealed that the dopant concentration was inhomogeneous, and suggested that the average concentration was ten times smaller than the nominal value. The constancy of the lattice constants and average concentration x_{av}(XRD) as determined by XRD for $0.3 < x_{nom} \leqslant 0.5$ is suggestive of a two-phase region, with $x_{nom} = 0.3$ as the maximum solubility. However, the bulk resistivity and specific heat vary systematically in this region of alloy parameter, with a monotonic evolution of the coherence temperature and superconducting transition temperature (see Figs. 2 and 3). This seems to indicate that the actual average alloy concentration increases

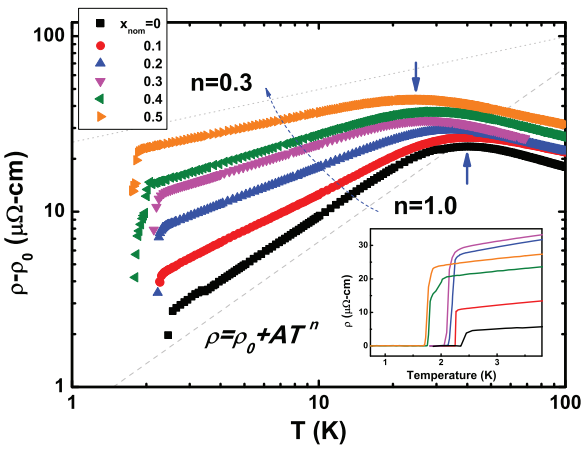

FIG. 2. (Color online) The temperature dependence of the resistivity of $Ce(Co_{1-x}Ru_x)In_5$ on a ln T scale. The residual resistivity ρ_0 (determined by fitting to the power law $\rho = \rho_0 + AT^n$) has been subtracted for all samples shown in the main panel. (Inset) The low-temperature resistivity on a linear scale, showing the rapid drop of the resistivity to zero at the superconducting transition.

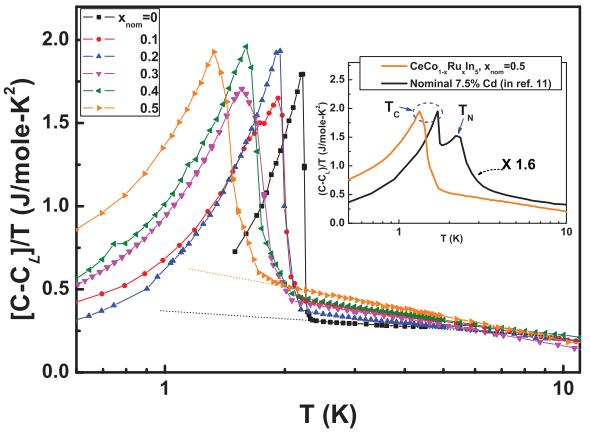

FIG. 3. (Color online) The temperature dependence of the electronic specific heat of $Ce(Co_{1-x}Ru_x)In_5$. The lattice contribution, determined from the specific heat of $LaCoIn_5$, has been subtracted from these results. The extrapolations of the normal state electronic specific heat for nominal concentrations $x_{nom} = 0$ and 0.5 are drawn in the figure to emphasize the increase of the electron specific heat coefficient with increasing x. (Inset) A comparison of the specific heat coefficient C/T vs T for a Ru-doped sample with $x_{nom} = 0.5$ and a Cd-doped sample with a similar T_c; the latter shows magnetic order, the former does not [data for $CeCo(In_{5-x}Cd_x)$ are from Ref. 17].

as x_{nom} increases and that our bulk measurements accurately reflect the behavior at the average concentration. For samples with nominal $x_{nom} = 0.2$, 0.4, and 0.5 the microprobe analysis and single crystal x-ray diffraction were performed on various regions of the same samples used for the resistivity and specific heat. The most likely explanation of the disparities in the actual alloy concentration deduced from these measurements is that the stoichiometry varied in the different regions of the inhomogeneous samples that were examined in each separate experiment; another possibility is that etching the samples in 20% HCl/80% H_2O mixture prior to the EDX measurement changed the Ru concentration near the surface. Measurements of the electrical resistivity and heat capacity were performed using a commercial Quantum Design PPMS-9 with a ^{3}He-PPMS insert. For the electrical resistivity, platinum wires were spot welded onto one side of the crystal plate for the four wire (ac) measurement. The heat capacity was measured using a thermal relaxation method.

III. RESULTS AND DISCUSSION

The results for the electrical resistivity are shown in Fig. 2 on a log-log scale; the curves have been shifted vertically to clarify the change in the low-temperature power-law behavior. All the curves show behavior typical of heavy Fermion materials. At high temperatures, $d\rho/dT$ is negative, indicative of Kondo behavior. A pronounced maximum of the resistivity occurs at a temperature T^*, which we interpret as the coherence temperature. In contrast to electron doping by Pt or Sn substitution, where T^* increases with alloying,[16] for hole doping with Ru the coherence temperature decreases as the concentration increases, from 41 K at $x_{nom} = 0$ to 25 K at $x_{nom} = 0.5$. This trend is exhibited in Fig. 4(a). The decrease

of T^* as x increases, which is also observed for Cd substitution, suggests that the electron ground state approaches a QCP for a transition to antiferromagnetism with increasing hole doping, while electron doping pushes the system away from quantum criticality towards a paramagnetic state.[5,16,17,20] At lower temperatures, the behavior of the resistivity evolves from a linear to a sublinear temperature dependence as the Ru concentration increases. We do not know the origin of this behavior, but find it interesting that both electron doping (Sn or Pt) and hole doping (Cd and Ru) cause the resistivity to become sublinear although the dopants have the opposite effect on the magnetic criticality.

As seen in the inset of Fig. 2, at sufficiently low temperature the resistivity of these alloys drops rapidly to zero. We assign the temperature at the midpoint between the normal and zero-resistivity states as the superconducting transition temperature $T_{\text{c-mid}}$; this equals 2.3 and 1.72 K for $x_{\text{nom}} = 0$ and 0.5, respectively. We note that both T^* and T_c follow the same trend in that they are suppressed monotonically with Ru alloying [see Figs. 4(a) and 4(b)]. [The error bars in Fig. 4(b) are determined from the temperatures where the resistivity falls to 90% and 10% of its normal state value.]

Due to an uncertainty in the small masses of our samples, we have normalized the specific heat of all our alloys to the specific heat of undoped Co115 at 20 K. The results for the low-temperature electronic specific heat for all our $Ce(Co_{1-x}Ru_x)In_5$ samples are shown in Fig. 3 as C/T versus T. A lattice contribution (C_L) determined from that of $LaCoIn_5$ has been subtracted from this data. The decrease of the SC transition temperature (T_c) with increasing Ru concentration is similar to that seen for $T_{\text{c-mid}}$ in the resistivity $\rho(T)$. [The error bars in Fig. 4(b) are determined by linear interpolation of the data from the peak in the specific heat to the normal state linear behavior.] The increase of the linear coefficient as x_{nom} increases is also consistent with the decrease in T^* as the system approaches an AFM QCP. Unlike the case of Cd doping, however, there is no obvious extra peak arising from an AFM transition at any concentration we have studied (see Fig. 3 inset).

Gofryk *et al.*[16] have pointed out that all dopants of $CeCoIn_5$ have both a pair breaking effect and an electronic tuning effect. Electron doping with Sn or Pt increases the coherence temperature T^*, decreases the linear coefficient of specific heat, and drives the system away from an AFM QCP toward a paramagnetic state, while hole doping with Cd and Hg has the reverse effect, pushing the system towards an AFM state. These authors also point out that the rate of suppression of the SC T_c is similar for electron doping, whether via Sn onto the In sites or via Pt onto the Co buffer layer ($dT_c/dx = -11.3\ \text{K}/x_{\text{Pt}}$, $-13.2\ \text{K}/x_{\text{Sn}}$). While the initial suppression of T_c for Cd doping is similar [$dT_c/dx = -12.8\ \text{K}/x_{\text{Cd}}$, see Fig. 4(c)], if the decrease of T_c is compared to the change in the scattering rate on alloying, it is found that the pair breaking effect is weaker for the hole dopants Cd and Hg[16] than for the electron dopants.

In the absence of a precise determination of the actual alloy concentrations for Ru doping, it is difficult to make comparisons with these other dopants. However, the most significant comparison between Ru and Cd doping is that no AFM transition is observed for the former dopant for values of T_c comparable to those for Cd doping where the co-existence

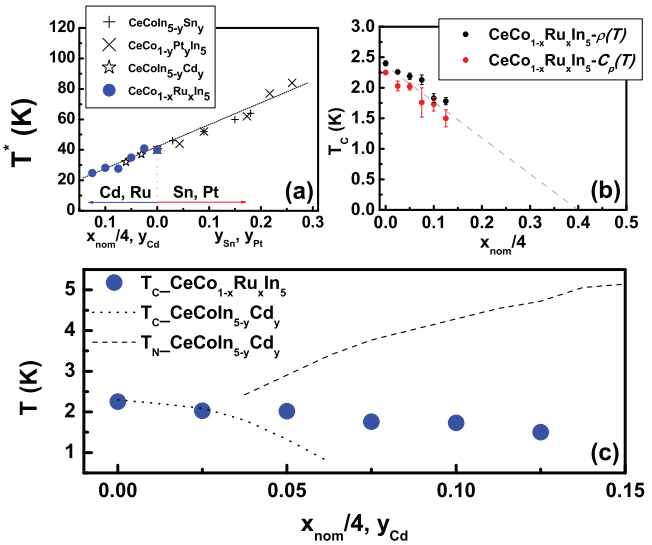

FIG. 4. (Color online) The maximum temperature T^* of the resistivity of $Ce(Co_{1-x}Ru_x)In_5$ as a function of alloy concentration compared to the values observed for Sn, Pt, and Cd dopants. (b) The superconducting transition temperatures T_c as estimated by the midpoint $T_{\text{c-mid}}$ of the resistive transition and from an equal area construction on the specific heat. (c) Comparison of the effects of Ru and Cd doping on the phase diagram. The dashed and dotted lines stand for the AFM Néel temperature (T_N) and the SC transition temperature (T_c) for Cd dopants,[17] respectively, while the solid circles represent T_c for Ru dopants. In these plots, we have divided the nominal concentration of Ru by a factor of 4, which corresponds to the assumption that the actual Ru concentration is determined by the behavior of T^*.

of an AFM transition is clear (see Fig. 3 inset). This allows us to speculate on two possible scenarios.

In the first case, we assume that the value of T^* allows us to determine the actual doping concentration x_{act} for Ru. This is based on the observation that for Sn, Pt, and Cd doping T^* scales linearly with the electron count [see Fig. 4(a)] independent of the dopant atom.[16] In this case, x_{act} has the same value as for $CeCo(In_{5-x}Cd_x)$ at the same value of T^*, and one finds that $x_{\text{act}} = x_{\text{nom}}/4$, similar to the relation deduced from refinement of single crystal XRD profiles. This results in a very weak suppression for superconductivity $dT_c/dx_{\text{Ru}} = -7\ \text{K}/x_{\text{Ru}}$, which is roughly half that found for electron or La dopants.[16,21] As can be seen in Fig. 4(c), the suppression of T_c under this hypothesis is clearly weaker than for Cd-doped Co115; indeed, the critical concentration x_c for suppression of superconductivity is comparable to that seen for Pt or Sn doping, where $x_c \sim 0.2$. However, the absence of long-range order seen in Fig. 4(c) is stunning in comparison to the Cd doped samples. Under the given assumption, we would have anticipated a magnetic ordering temperature for our sample with the largest Ru doping to be greater than 4 K, which is clearly not observed. Thus, in this scenario, there is a clear difference in the ability to establish long-range magnetic order with Ru doping in comparison to Cd (or Hg) doping; otherwise said, the critical concentration for the AF QCP is more than a factor of two larger for Ru doping than for Cd doping.

In the second scenario, we assume that the ability to generate long range magnetic order is determined solely by the nominal electron count. In this case, x_{act} has the same value as for $CeCo(In_{5-x}Cd_x)$ at the same value of T_N. This scenario is supported by the fact that when Sn- and Pt-doped samples are co-doped with Hg, they have the same Néel temperature when the electron count is identical.[16] Under this assumption, the actual Ru doping at $x_{nom} = 0.5$ must be less than $x_{act} = 0.03$ where antiferromagnetism first appears for Cd doping so that the actual concentration must be at least fifteen times smaller than the nominal value, consistent with the average concentration deduced from the EDX. For this hypothesis, the coherence temperature T^* no longer simply scales with the electron count, and T_c is smaller than for Cd doping at the same concentration so that the pair breaking strength for Ru dopants is stronger than for Cd (or Hg) dopants.

In either case, we come to the conclusion that Ru and Cd dopants produce significant differences in the electronic tuning and/or the superconducting pair breaking response. It is not clear which scenario represents reality, but we can say with certainty that a difference exists between Ru and Cd doping that was not observed in the case of Sn and Pt doping. Since there is no change in lattice constant when Co115 is doped with Cd or Sn, while the lattice initially expands on Ru doping, it is possible that the additional negative chemical pressure effect induced by Ru doping influences this difference. This explanation, however, appears to be contradicted by the saturation of the lattice constants for $x_{nom} > 0.3$. A second possibility is that Ru doping affects the electronic structure throughout the bulk, while Cd doping affects only the nearby Ce atoms. Such a local effect, which has been proposed for Cd doping based on NMR measurements,[22] appears to contradict the fact that T^* and T_c for Cd doped samples can be reversibly tuned by application of pressure[17] or by co-doping with Pt or Sn.[16] Finally, it should be mentioned that hole doping via alloying Yb onto the Ce site leads to no change in the Ce valence or coherence temperature T^* and a linear decrease in T_c towards $T = 0$ at $YbCoIn_5$ suggesting that alloying with Yb leads merely to simple dilution effects.[14,23] This serves as a warning that the phase diagram of Fig. 4 may not be a comparable function of electron count as is seen for other dopants.

IV. SUMMARY

In summary, we have synthesized $Ce(Co_{1-x}Ru_x)In_5$ crystals using In flux growth. Doping $CeCoIn_5$ with Ru causes a decrease of the coherence temperature T^*, the onset of a sub-linear temperature dependence in the resistivity, and the suppression of the SC T_c. These results imply that hole doping via Ru alloying moves the system towards an AFM ground state. Finally, the absence of AFM at our highest Ru concentration gives a hint of different physics for Ru doping in $CeCoIn_5$ than for Cd or Hg doping.

ACKNOWLEDGMENTS

This work was supported in part by project no. NSC 100-2112-M-001-019-MY3 of the National Science Council, Taiwan. Work at Los Alamos National Laboratory was performed under the auspices of the U.S. DOE, Office of Basic Energy Sciences, Division of Materials Sciences and Engineering. Work at the University of Alberta was supported by the Natural Sciences and Research Council of Canada.

*oumn@phys.sinica.edu.tw
†cheny2@phys.sinica.edu.tw

[1] C. M. Varma, Z. Nussinov, and W. v. Saarloos, Phys. Rep. **361**, 267 (2002).
[2] H. v. Löhneysen, J. Phys.: Condens. Matter **8**, 9689 (1996).
[3] N. D. Mathur, F. M. Grosche, S. R. Julian, I. R. Walker, D. M. Freye, R. K. W. Haselwimmer, and G. G. Lonzarich, Nature (London) **394**, 39 (1998).
[4] R. T. Macaluso, J. L. Sarrao, P. G. Pagliuso, N. O. Moreno, R. G. Goodrich, D. A. Browne, F. R. Fronczek, and J. Y. Chan, J. Solid State Chem. **166**, 245 (2002).
[5] P. G. Pagliuso, R. Movshovich, A. D. Bianchi, M. Nicklas, N. O. Moreno, J. D. Thompson, M. F. Hundley, J. L. Sarrao, and Z. Fisk, Physica B **312–313**, 129 (2002).
[6] V. S. Zapf, E. J. Freeman, E. D. Bauer, J. Petricka, C. Sirvent, N. A. Frederick, R. P. Dickey, and M. B. Maple, Phys. Rev. B **65**, 014506 (2001).
[7] C. Petrovic, P. G. Pagliuso, M. F. Hundley, R. Movshovich, J. L. Sarrao, J. D. Thompson, Z. Fisk, and P. Monthoux, J. Phys.: Condens. Matter **13**, L337 (2001).
[8] G. Sparn, R. Borth, E. Lengyel, P. G. Pagliuso, J. L. Sarrao, F. Steglich, and J. D. Thompson, Physica B **312–313**, 138 (2002).
[9] S. Nakatsuji, D. Pines, and Z. Fisk, Phys. Rev. Lett. **92**, 016401 (2004).
[10] M. A. Tanatar, J. Paglione, S. Nakatsuji, D. G. Hawthorn, E. Boaknin, R. W. Hill, F. Ronning, M. Sutherland, L. Taillefer, C. Petrovic, P. C. Canfield, and Z. Fisk, Phys. Rev. Lett. **95**, 067002 (2005).
[11] S. K. Goh, J. Paglione, M. Sutherland, E. C. T. OFarrell, C. Bergemann, T. A. Sayles, and M. B. Maple, Phys. Rev. Lett. **101**, 056402 (2008).
[12] E. D. Bauer, Yi-feng Yang, C. Capan, R. R. Urbano, C. F. Miclea, H. Sakai, F. Ronning, M. J. Graf, A. V. Balatsky, R. Movshovich, A. D. Bianchi, A. P. Reyes, P. L. Kuhns, J. D. Thompson, and Z. Fisk, Proc. Natl. Acad. Sci. USA **108**, 6857 (2011).
[13] J. Panarin, S. Raymond, G. Lapertot, J. Flouquet, and J.-M. Mignot, Phys. Rev. B **84**, 052505 (2011).
[14] L. Shu, R. E. Baumbach, M. Janoschek, E. Gonzales, K. Huang, T. A. Sayles, J. Paglione, J. O'Brien, J. J. Hamlin, D. A. Zocco, P.-C. Ho, C. A. McElroy, and M. B. Maple, Phys. Rev. Lett. **106**, 156403 (2011).
[15] J. Paglione, T. A. Sayles, P. C. Ho, J. R. Jeffries, and M. B. Maple, Nat. Phys. **3**, 703 (2007).
[16] K. Gofryk, F. Ronning, J. X. Zhu, M. N. Ou, P. H. Tobash, S. S. Stoyko, X. Lu, A. Mar, T. Park, E. D. Bauer, J. D. Thompson, and Z. Fisk, Phys. Rev. Lett. **109**, 186402 (2012).

[17]L. D. Pham, T. Park, S. Maquilon, J. D. Thompson, and Z. Fisk, Phys. Rev. Lett. **97**, 056404 (2006).

[18]E. D. Bauer, F. Ronning, C. Capan, M. J. Graf, D. Vandervelde, H. Q. Yuan, M. B. Salamon, D. J. Mixson, N. O. Moreno, S. R. Brown, J. D. Thompson, R. Movshovich, M. F. Hundley, J. L. Sarrao, P. G. Pagliuso, and S. M. Kauzlarich, Phys. Rev. B **73**, 245109 (2006).

[19]E. D. Bauer, N. O. Moreno, D. J. Mixson, J. L. Sarrao, J. D. Thompson, M. F. Hundley, R. Movshovich, and P. G. Pagliuso, Physica B **359–361**, 35 (2005).

[20]C. H. Booth, E. D. Bauer, A. D. Bianchi, F. Ronning, J. D. Thompson, J. L. Sarrao, J. Y. Cho, J. Y. Chan, C. Capan, and Z. Fisk, Phys. Rev. B **79**, 144519 (2009).

[21]C. Petrovic, S. L. Budko, V. G. Kogan, and P. C. Canfield, Phys. Rev. B **66**, 054534 (2002).

[22]R. R. Urbano, B.-L. Young, N. J. Curro, J. D. Thompson, L. D. Pham, and Z. Fisk, Phys. Rev. Lett. **99**, 146402 (2007).

[23]C. H. Booth, T. Durakiewicz, C. Capan, D. Hurt, A. D. Bianchi, J. J. Joyce, and Z. Fisk, Phys. Rev. B **83**, 235117 (2011).